



GEOLOGY OF MINERAL DEPOSITS

Research paper

<https://doi.org/10.17073/2500-0632-2025-03-386>

UDC 553.43/.44:553.065(597)

**Geological and isotopic constraints on the copper ore formation in Ta Phoi area, Lao Cai province, Northwestern Vietnam**K. T. Hung¹   , N. X. Dac²¹ Hanoi University of Mining and Geology, Hanoi, Vietnam² Vietnam Institute of Geosciences and Mineral Resources, Hanoi, Vietnam khuongthehung@humg.edu.vn**Abstract**

The Ta Phoi copper deposit, located in the northeastern Phan Si Pan zone, Northwestern Vietnam, is a significant site of Neoproterozoic Cu mineralization. Its distinct geological characteristics justify its investigations, especially in comparison to nearby IOCG Sin Quyen deposit. This study is aimed at clarifying the genesis, ore-forming conditions, and fluid evolution of the Ta Phoi deposit through an integrated approach combining geological, petrographic, geochemical, and isotopic data analysis. The research specifically employs U-Pb dating of sphene, sulfur isotope analysis, and fluid inclusion microthermometry to identify the age, origin, and physicochemical environment of the mineralization. Sphene U-Pb dating yielded concordant ages of 810.7 ± 4.6 Ma and 819.5 ± 2.0 Ma, indicating a Neoproterozoic mineralization event temporally linked to regional granodiorite and diorite intrusions. Sulfur isotope values ($\delta^{34}\text{S} = +2.2$ to $+3.1\text{‰}$) suggest a magmatic origin for ore-forming fluids. Fluid inclusion data detected fluid temperatures ranging from 163.1°C to 410°C , fluid salinities of 2.1–16.25 wt% NaCl equiv., and formation pressures of 44–100 MPa at depths of 3.4–6.5 km. These results confirmed that the Ta Phoi deposit formed from medium- to high-temperature, magmatogene hydrothermal fluids in a subduction-related continental arc setting; it may represent a porphyry-related skarn or endoskarn system that developed in response to magmatic fluid migration along lithological contacts and faults. These findings provide new insights into the metallogenic framework of the Ta Phoi deposit and highlight its potential for further Cu exploration in Northwestern Vietnam.

Keywords


Copper ore, U-Pb dating, sphene, metallogeny, Ta Phoi deposit, North-Western Vietnam

For citation

Hung K. T., Dac N. X. Geological and isotopic constraints on the copper ore formation in Ta Phoi area, Lao Cai province, Northwestern Vietnam. *Mining Science and Technology (Russia)*. 2025;10(3):262–279. <https://doi.org/10.17073/2500-0632-2025-03-386>

ГЕОЛОГИЯ МЕСТОРОЖДЕНИЙ ПОЛЕЗНЫХ ИСКОПАЕМЫХ

Научная статья

Геологические и изотопные оценки условий образования медных руд в районе Та Фой, провинция Лао Кай, северо-западный ВьетнамХ. Т. Хунг¹   , Н. С. Дак²¹ Ханойский университет горного дела и геологии, г. Ханой, Вьетнам² Вьетнамский институт наук о Земле и минеральных ресурсов, г. Ханой, Вьетнам khuongthehung@humg.edu.vn**Аннотация**

Месторождение меди Та Фой (Ta Phoi), расположенное в северо-восточной части зоны Фан Си Пан на северо-западе Вьетнама, является важным объектом проявления неопротерозойской медной минерализации. Его отличительные геологические характеристики оправдывают его изучение, особенно в сопоставлении с близлежащим месторождением типа Fe-оксидных Au-Cu гидротермальных месторождений (IOCG) Синь Куен (Sin Quyen). Цель данного исследования – выявить генезис, условия рудообразования и эволюцию флюидов месторождения Та Фой с помощью комплексного подхода, сочетающего анализ геологических, петрографических, геохимических и изотопных данных. В частности, в исследовании используются U-Pb датирование сфена, изотопный анализ серы и микротермометрия флюидных включений для определения возраста, происхождения и физико-химических условий формирования минерализации. Определение возраста сфена U-Pb методом дало согласующиеся возрасты $810,7 \pm 4,6$ млн лет и $819,5 \pm 2,0$ млн лет, что указывает на неопротерозойский возраст минерализации, совпадающий с возрастом региональных гранодиоритовых и диоритовых интрузий. Изотопный анализ серы ($\delta^{34}\text{S} = +2,2$ до $+3,1\text{‰}$) указывает на магматическое происхождение рудообразующих флюидов. Данные по флюидным включениям показали,



что температура флюидов колебалась от 163,1 °C до 410 °C, солёность флюидов составляла 2,1–16,25 вес. % в эквиваленте NaCl, а пластовое давление – 44–100 МПа на глубине 3,4–6,5 км. Эти результаты подтвердили, что месторождение Та Фой образовалось в результате воздействия магматогенных гидротермальных флюидов средней и высокой температуры в субдукционных условиях континентальной дуги; оно может представлять собой порфировую скарновую или эндоскарную систему, которая сформировалась в результате миграции магматических флюидов вдоль литологических контактов и разломов. Эти результаты дают новое представление о металлогенической обстановке формирования месторождения Та Фой и подчеркивают потенциал дальнейшей разведки на медь в северо-западной части Вьетнама.

Ключевые слова

медная руда, U-Pb определение возраста, сфен, металлогения, месторождение Та Фой, северо-западный Вьетнам

Для цитирования

Hung K. T., Dac N. X. Geological and isotopic constraints on the copper ore formation in Ta Phoi area, Lao Cai province, Northwestern Vietnam. *Mining Science and Technology (Russia)*. 2025;10(3):262–279. <https://doi.org/10.17073/2500-0632-2025-03-386>

Introduction

The mineralization process typically occurs over a wide spatial range and is closely associated with deformation, metamorphism, faulting, and magmatic intrusion events during specific tectonic stages. These processes contribute to the formation of significant mineral deposits, containing copper (Cu), gold (Au), lead (Pb), zinc (Zn), and rare earth elements (REE), along with other associated minerals [1–3].

Lao Cai province located in the Phan Si Pan zone in northwestern Vietnam has significant mineral resource potential, particularly as for Cu-Au mineralization, which has been assessed as highly prospective [4]. Consequently, in 2015, the Vietnam government approved the establishment of the Lao Cai copper metallurgical industrial zone, with a processing capacity exceeding 10,000 tons of cathode copper/year. Geological mapping and mineral exploration conducted along the northeastern margin of the Phan Si Pan zone have identified several large copper ore deposits, including the Sin Quyen, Ta Phoi, and Vi Kem deposits, as well as valuable copper mineralization occurrences such as Nam Chac, Trinh Tuong, Lung Thang, and Lung Po [5–9]. However, these studies remain fragmented, lack in-depth analysis, and have yet to incorporate modern mineralization research techniques. In recent years, some studies on mineralization have focused on copper deposits in Lao Cai area, first of all, the Sin Quyen deposit [10–12]. These investigations have introduced new perspectives on the nature and formation age of copper mineralization in the northeastern Phan Si Pan zone, particularly at the Sin Quyen deposit, revealing the presence of gold and rare earth elements (REE) alongside copper as major economic commodities [13]. This raises the question of whether deposits with economic significance, similar to Sin Quyen, exist along the Lung Po–Ta Phoi metallogenic belt. The Ta Phoi copper deposit within this belt has been estimated to contain substantial copper re-

serves [14, 15], but its potential for associated gold and REE mineralization remains uncertain. Furthermore, the genetic mechanisms of ore formation at Ta Phoi and Sin Quyen require clarification – do they share similar mineralization processes and metallogenic periods? Addressing these questions necessitates comprehensive research into the material composition, formation conditions, spatial distribution, and genesis of the mineralization. Such studies would provide a scientific basis for more precise mineral exploration strategies and resource estimation in the region.

The **aim** of this study is to clarify the geological and isotopic features of copper ore formation in the Ta Phoi area through an integrated analysis of field observations, petrography, and geochemical data.

To achieve this aim, the study was focussed on the following key **tasks**:

- characterizing geological setting and lithological units that host copper mineralization;
- analyzing petrographic features and mineral assemblages to interpret alteration patterns and paragenetic sequences;
- integrating U-Pb sphene geochronology to constrain the mineralization formation timing;
- applying sulfur isotope analysis to identify the source of ore-forming materials;
- conducting fluid inclusion studies to determine the temperature, salinity, pressure, and depth conditions of ore formation.

The outcomes of this research will enhance the understanding of metallogenic processes in the region and provide valuable insights for future mineral exploration in northwestern Vietnam.

1. Geological setting

Northwestern Vietnam belongs to the South China and Indochina blocks (Figs. 1, *a*, *b*). These blocks are integral components in the palaeogeographic reconstruction of the Rodinia supercontinent [16–19]. Several copper deposits, including the Iron Oxide

Copper-Gold (IOCG) deposits of Sin Quyen, and copper Suoi Thau, Ta Phoi, are located in Northwestern Vietnam (Fig. 1, c).

The Ta Phoi copper deposit is located in the northwestern Vietnam, which is bordered by the Song Chay fault to the north and the Song Ma belt to the south [4]. This region comprises three major tectonic units: the Phan Si Pan zone, the Song Da rift, and the Tu Le basin (Fig. 2, a). The Song Da rift is an elongated, northwest-southeast trending structure characterized by Devonian to Middle Triassic sedimentary-volcanic sequences. A prominent feature of this rift is the well-developed Permian-Triassic alkaline basalts (~260 Ma), which predominantly occur along the Da River [24]. These basalts, along with silicic volcanic rocks, rest atop Early Permian limestone and are subsequently overlain unconformably by Triassic limestone and schist containing coal deposits [25, 26]. Some studies suggest that the Song Da volcanic suite is linked to the Emeishan plume [27–29]. The Tu Le Basin is predominantly composed of rhyolite, trachy-

rhyolite, and trachydacite. Zircon U-Pb dating indicates that the rhyolites in this basin formed during the Late Permian (262–252 Ma), contemporaneously with the mafic rocks of the Song Da Rift [30, 31].

The Phan Si Pan zone serves as a tectonic link between two major crustal blocks: the North Vietnam–South China block and the Indochina block (Fig. 2, b). It is positioned between the Red River shear zone and the Tu Le basin and is composed primarily of Mesoarchean to Early Paleoproterozoic basement rocks, including biotite quartzite, quartz-biotite-garnet schist, and amphibolite [23, 33]. Paleo-Mesoproterozoic units in the zone consist of biotite schist, two-mica schist, and amphibolite [23, 33]. Precambrian magmatism in the Phan Si Pan zone is characterized by several granitoid and mafic intrusive events, including: Mesoarchean granitoids (2.9–2.8 Ga) [33–35], Paleoproterozoic granitoids (1.8–2.2 Ga) [33, 35–37], Paleoproterozoic mafic dykes (1.8–2.3 Ga) [33], and Neoproterozoic granitoids (760–751 Ma) [20, 21, 23, 38].

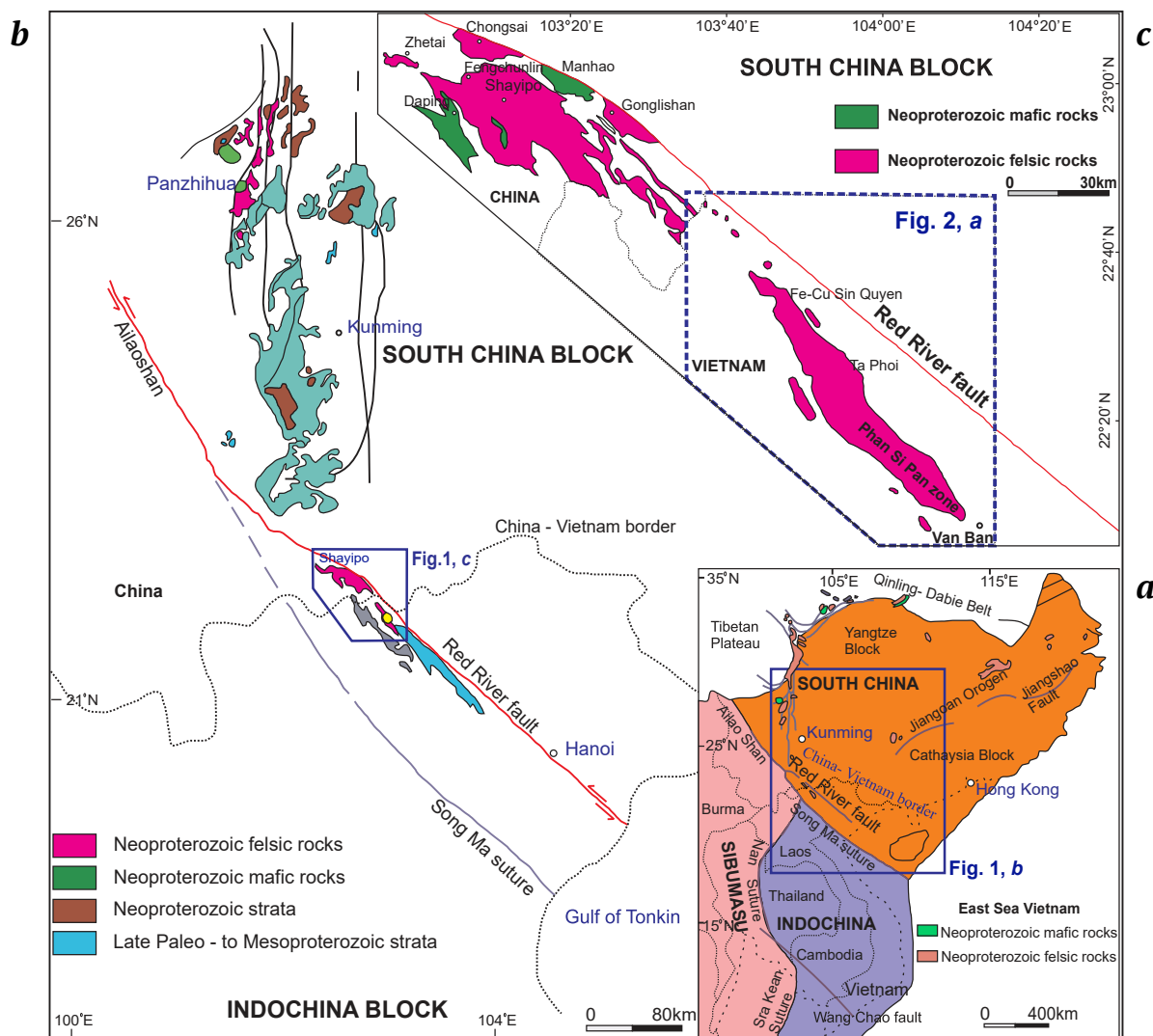


Fig. 1. Simplified tectonics map of NW Vietnam and adjoining areas ([20–23] and references therein)

The Mesoproterozoic–Paleoproterozoic crystalline basement is unconformably overlain by Paleozoic–Mesozoic meta-sedimentary and sedimentary sequences, which include quartz-sericite-chlorite schist, quartzite, limestone, and dolomite (see Figs. 2, *a, b*). In addition to the Precambrian granitoids, voluminous A-type granites intruded during the Late Permian–Early Triassic, closely associated with the Emeishan mantle plume [29–31, 39]. Cenozoic plutons have also been identified in the region [40, 41].

The Neoproterozoic granitoid intrusions in the Phan Si Pan zone include the Po Sen, Phin Ngan, and Lung Thang plutons, along with several smaller bodies and lenses (Fig. 2, *b*) [42]. These intrusions are comparable to the widespread Neoproterozoic granitoids (~860–740 Ma) in the western and southwestern Yangtze Block (see Fig. 1) [42–47].

2. Geology of the Ta Phoi deposit

2.1. Stratigraphy and Lithology

The Ta Phoi copper deposit is located in Ta Phoi area, Lao Cai Province, covering an area of approximately 4 km². The deposit occurs in the northeastern limb of the Hoang Lien Son anticlinorium, within the Phan Si Pan structural zone. It is primarily composed of metamorphosed sedimentary suites of the Sin Quyen Formation, along with small undated intrusive bodies situated adjacent to the large intrusive mass of the Po Sen Complex. The deposit is primarily hosted in metamorphic rocks of the second unit of the Sin Quyen Formation (PPsq₂), which is a key geological factor closely associated with copper ore formation in the study area [4, 14].

The second unit of the Sin Quyen Formation is widespread in the Ta Phoi area and consists of quartz-feldspar-biotite schist, metasomatic rocks, amphibolite lenses, and graphite-bearing quartz-mica schist. The feldspar-quartz-biotite schist contains small amount to no graphite, exhibits a brown color, schistose structure, and lepidoblastic texture. Muscovite-sericite minerals (1–8%) are commonly enriched along orebody margins and fault zones. Accessory minerals include sphene, apatite, epidote, zoisite, and ore minerals.

The metasomatic rocks occur as bands in the central part of the area, while amphibolite appears as lenticular bodies within the metasomatic rocks, characterized by an opaque white color, interbedded with greenish layers. Amphibolite is commonly found along the hanging walls of copper ore bodies. The graphite-bearing quartz-mica schist is gray and exhibits a schistose structure. Copper mineralization is primarily hosted in metasomatic rocks, with lesser occurrences in feldspar-quartz-biotite schist. The second unit has a thickness exceeding 800 m (Figs. 3, *a–d*).

2.2. Igneous rocks

Granitoid formations of the Po Sen complex and granodiorite, diorite intrusions are widespread in the Ta Phoi area, along with the presence of lamprophyre dikes. Rocks of the Po Sen complex are distributed along the western and southwestern margins of the area, mainly represented by phase 2 and phase 3. Phase 2 consists of biotite granite and biotite-hornblende granite, while Phase 3 is characterized by light-colored dike rocks, including aplite granite and pegmatitic granite.

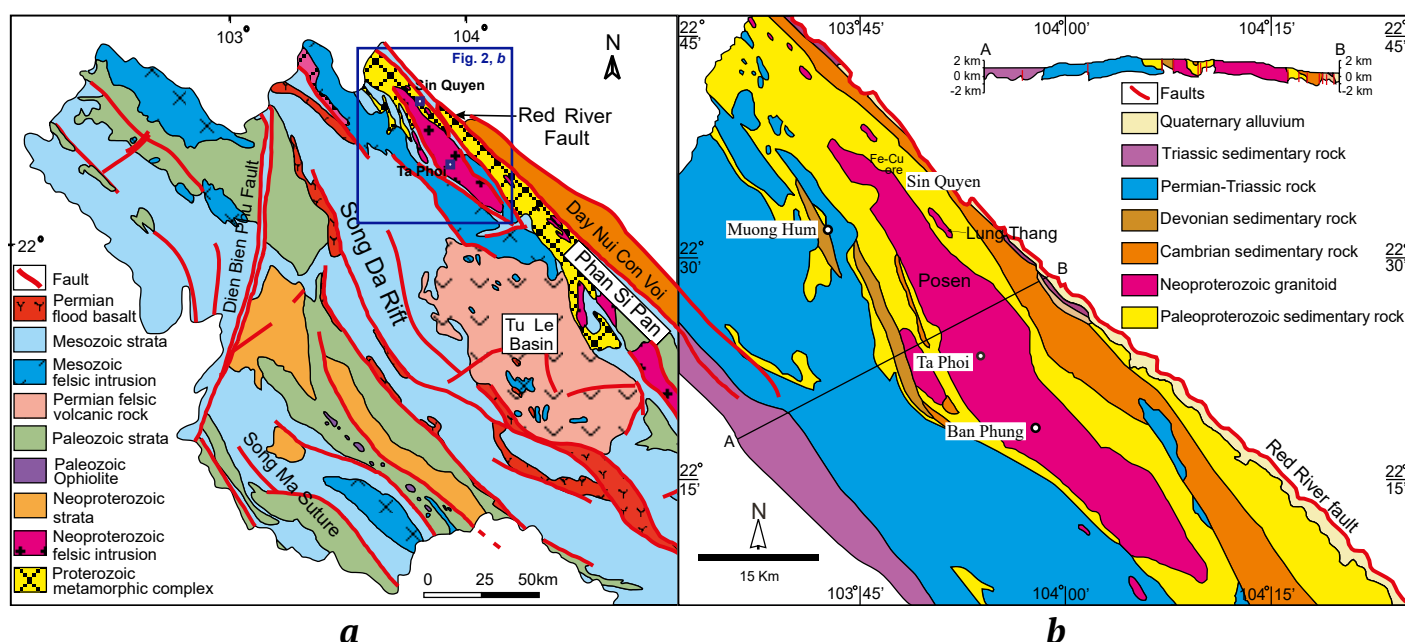


Fig. 2. Geological map of (a) northwestern Vietnam and (b) the Phan Si Pan zone and showing location of the Ta Phoi deposit (modified after [32])

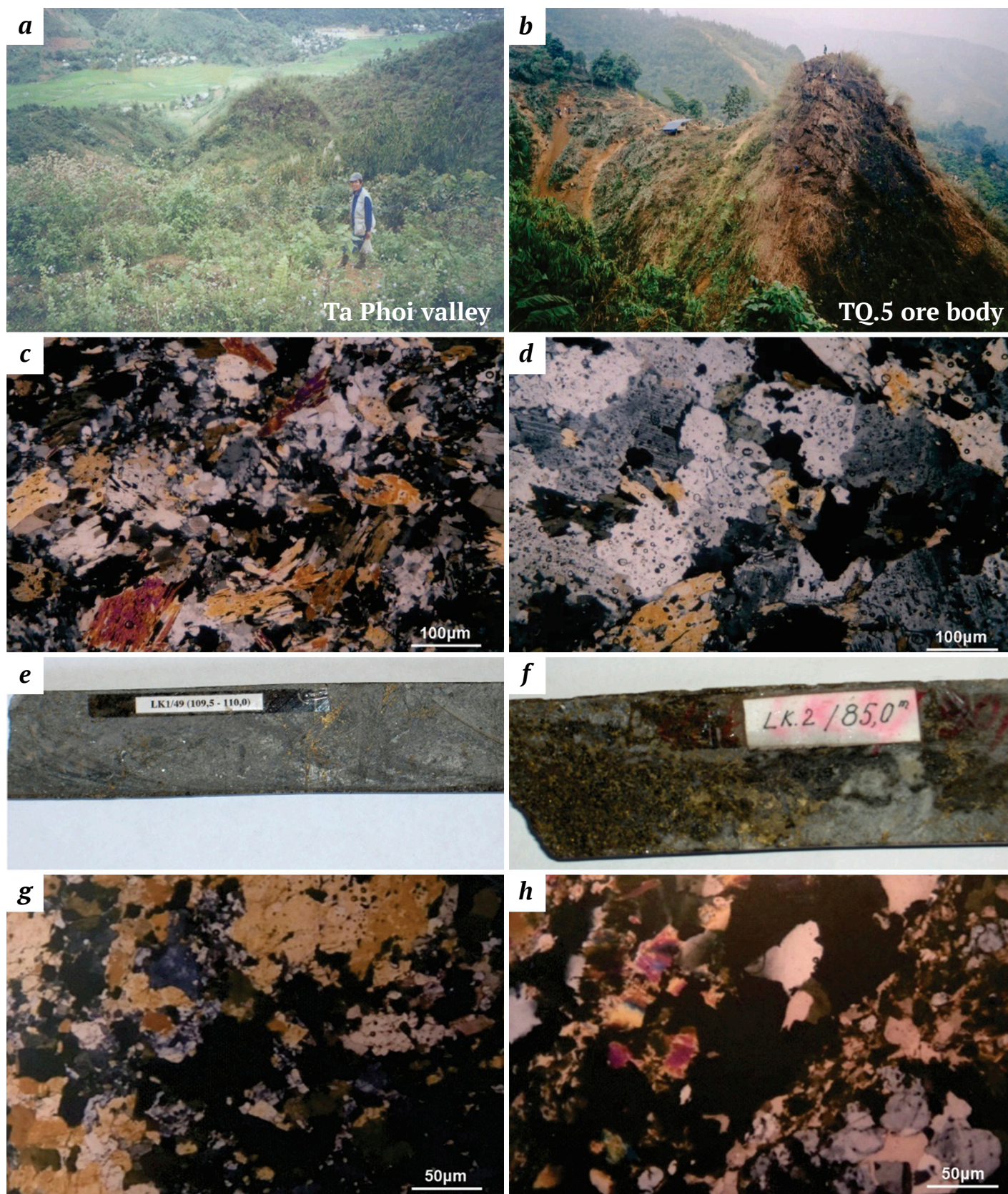


Fig. 3. Geological structure and material composition of the Ta Phoi deposit:

a, b – general view of the Ta Phoi valley and mining operations at the TQ.5 ore body (photo from [14]);

c, d – photomicrographs of rocks in transmitted light (magnification 35×, Nikon microscope): *c* – felsic schist (feldspar, quartz, biotite), drill core LK.2/28, depth 89–91 m; *d* – dark-colored metasomatic rock, drill core LK.1/13, depth 25–27 m (photo by Do Van Nhuan from [14]); *e–h* – manifestations of ore mineralization: *e, g* – disseminated ore in dark-colored metasomatic rock, drill core LK.1-T.1, depth 109.5–110 m; *f, h* – disseminated ore in felsic schist, drill core LK.2-T.1, depth 85 m (photo by Ly Quoc Su from [14])

U–Pb and $^{40}\text{Ar}/^{39}\text{Ar}$ dating methods have clarified the thermochronological history of the Po Sen complex. U–Pb analysis of composite samples of zircon grains by TIMS yielded an average age of 760 ± 25 Ma, clustering on the concordia line, while twelve SHRIMP U–Pb analyses provided a consistent age of 751 ± 7 Ma [38]. Combined with geochemical characteristics, these results indicate that the Po Sen complex is a Late Proterozoic magmatic complex.

Granodiorite and diorite rocks (namely Phin Ngan, Suoi Thau, Lung Thang massifs) are commonly found along the margins of ore bodies, with copper grades ranging from 0.01 to 0.4%. Copper mineralization within the diorite occurs as sparse dissemina-

tion and micro-veinlets along fractures. These rocks are gray to light gray, exhibit a massive structure, and have fine- to medium-grained textures, with localized weak deformation. Their crosscutting relationship with the surrounding rocks is unclear.

The absolute age dating results using the zircon U–Pb method for the granodiorite and diorite intrusions yielded ages of 776 ± 12 Ma for the Suoi Thau massif [48], 824 ± 4 Ma for the Phin Ngan massif [42], and 803 ± 3 Ma for the Lung Thang massif [47]. These results indicate that the formation of the granodiorite and diorite intrusions occurred during the Neoproterozoic. Moreover, most studies suggest that these intrusive bodies were generated in a subduction-related continental arc setting [42, 47, 48].

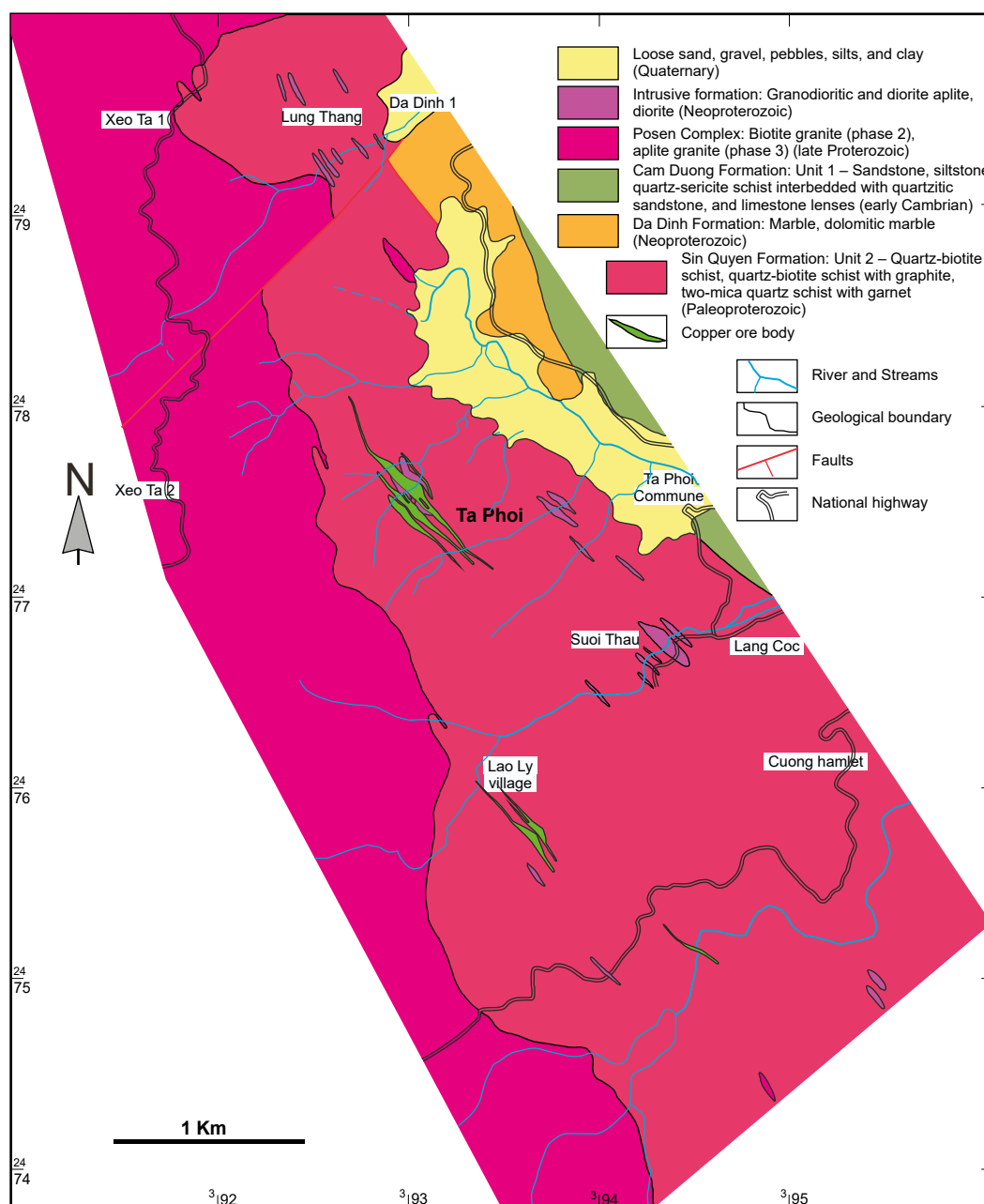


Fig. 4. Geological map of Ta Phoi area showing location of the Ta Phoi deposit (modified after [14])

Lamprophyre dikes intrude the surrounding rocks and are characterized by a grayish-green color, oriented structure, fine-grained texture and prismatic-granular texture. These dikes appear to have little to no association with copper mineralization.

2.3. Tectonics

The Ta Phoi ore deposit is located in the north-eastern limb of the Po Sen anticline, which exhibits a general monoclinic structure trending north-west-southeast and dipping to the northeast. Geological survey data indicate that surface rocks are strongly deformed, while drill core data reveal that at depth, both the host rocks and ore bodies maintain a consistent northeastward dip with dip angles ranging from 60 to 75° [4].

Along the Phoi 1 stream, a northwest-southeast trending fault, named Lang Phoi 1 Fault (F2), is observed. This fault is a subsidiary structure of the Ta Phoi Fault. The Lang Phoi 1 Fault cuts through and displaces rocks of the Sin Quyen Formation as well as biotite granite of the Po Sen Complex. Additionally, within the study area, the Ta Xeo 2 – Da Dinh Fault (F3) is identified. This fault extends along the Da Dinh

valley to Ta Xeo 2, with a total length of approximately 2.5 km. The Ta Xeo 2 – Da Dinh Fault displaces rock formations and intersects northwest-southeast trending faults [14] (Fig. 4).

2.4. Ore body distribution characteristics

The Ta Phoi copper deposit comprises 15 ore bodies, including lens-shaped and vein-type bodies. Among them, three large ore bodies (TQ.4, TQ.5, TQ.6) have been delineated, while the remaining 12 occur as smaller veins and lens-shaped clusters scattered throughout the area or along the margins of the larger ore bodies (TQ.1, TQ.2, TQ.3a, TQ.4a, TQ.7, TQ.8, TQ.9a, TQ.9b, TQ.10, TQ.10a, TQ.11, TQ.13) [14, 15]. These ore bodies dip northeastward at angle ranging from 60° to 85°, with strike length varying from 300 to 1200 m, thickness ranging from 1.5 to 94.8 m, and depths controlled up to 30–130 m. The primary ore minerals include chalcopyrite, cubanite, pyrite, and pyrrhotite, which exhibit irregular dissemination, occurring as isolated grains, clustered aggregates, or small ore pockets. These minerals also form veins filling microfractures and replacing pre-existing rock-forming minerals (Figs. 3, 5, Table 1).

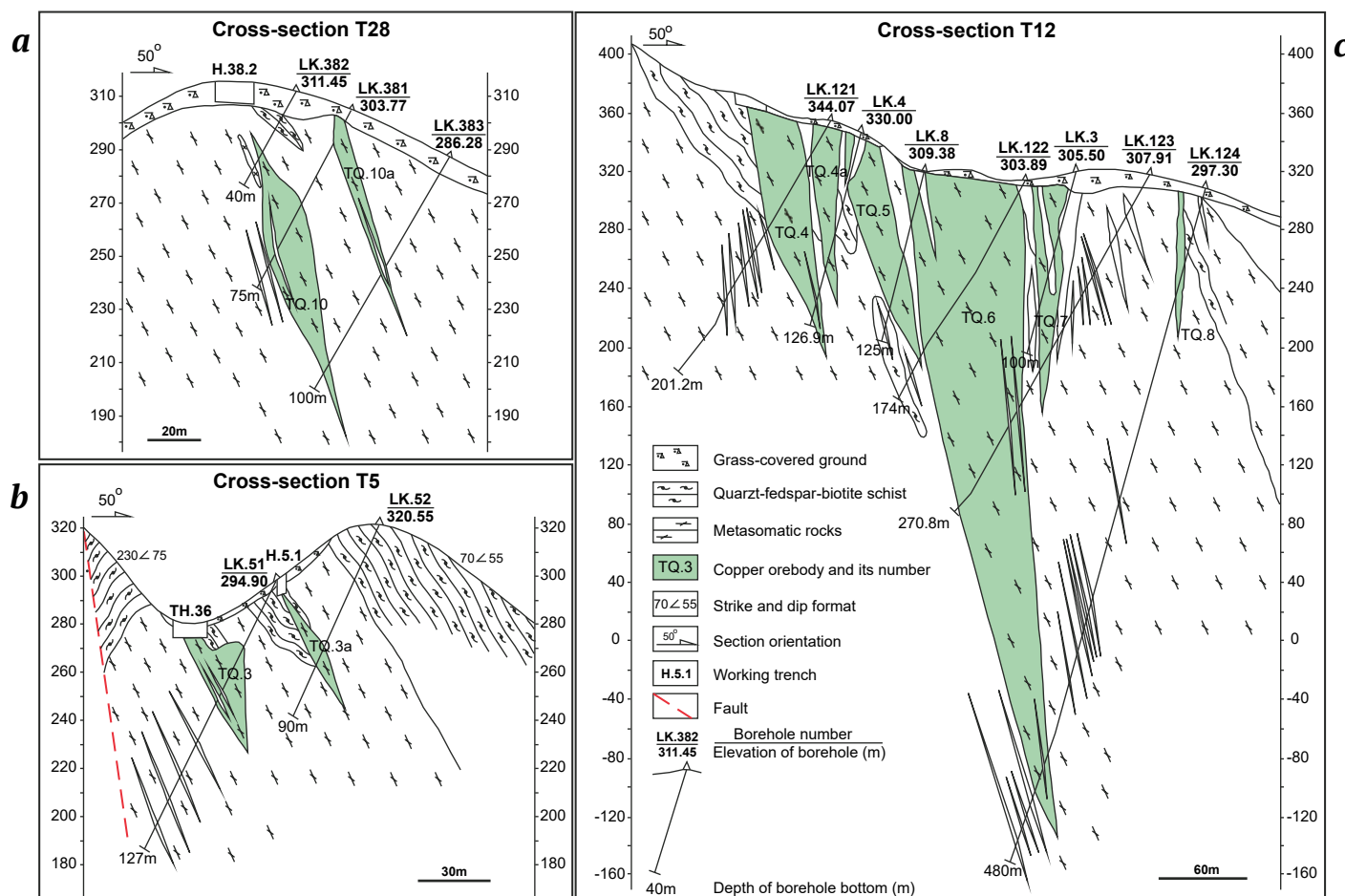


Fig. 5. Geological cross-sections along T5, T12, T28 lines showing TQ.3, TQ.3a, TQ.4, TQ.5, TQ.6, TQ.7, TQ.8 and TQ.10 orebodies [15]



2.5. Ore textures and structures

2.5.1. Types of ores and their properties

Petrographic and reflected light microscope analyses of copper ore samples from the study area reveal a complex assemblage of primary and secondary ore minerals. The primary sulfide minerals include chalcopryrite, bornite, pyrite, pyrrhotite, and cubanite,

while the secondary minerals such as covellite, chalcocite, malachite, and limonite occur as oxidation products in supergene alteration zones. Gangue minerals associated with the copper mineralization mainly comprise quartz and carbonate minerals.

Primary ore minerals include chalcopryrite, bornite, pyrite, pyrrhotite, cubanite, and magnetite.

Table 1

Morphological characteristics and composition of copper ore bodies in Ta Phoi deposit (after [14, 15])

Ore body number	Morphology of ore bodies	Length (m)	Dip direction	Dip angle	Average thickness (m)	Average copper grade (%)	Ore mineral composition
TQ.1	Vein	442	70°	65°	3.69	0.405	Pyrite 2%, chalcopryrite 1%, pyrrhotite 2%, marcasite in small amount, a arsenopyrite in small amount, rutin a few grains
TQ.2	Vein	300	65°	70°	2.00	0.447	Pyrite 3%, chalcopryrite in small amount, pyrrhotite 2%, graphite 1%, ilmenite in small amount
TQ.3a	Vein	210	60°	55°	12.05	0.455	Pyrite a few grains, chalcopryrite in small amount, covellite in small amount, graphite in small amount, ilmenite 1%
TQ.4	Large lense	580	50°	65°	21.04	0.698	Pyrite 1–2%, chalcopryrite 0.5–8%, pyrrhotite 10–55%, cuban-ite in small amount, graphite in small amount to 3%, covellite in small amount, molybdenite in small amount, gold 4–9 grains
TQ.4a	Vein	240	50°	65°	10.37	0.455	Pyrite 1%, chalcopryrite 8%, cubanite in small amount, covellite in small amount, mo-lybdenite in small amount
TQ.5	Large lense	830	50°	70°	16.56	0.638	Pyrite in small amount to 5%, chalcopryrite in small amount to 8%, pyrrhotite 1–12%, cubanite in very small amount to 1%, graphite in small amount, covellite in small amount, hem-atite a few grains
TQ.6	Large lense	597	60°	75°	16.39	0.835	Pyrite in small amount to 5%, chalcopryrite 1–10%, pyrrhotite in small amount to 8%, cubanite 1–10%, covellite in small amount to 3%, rutin a few grains, limonite in small amount to 5%, gold 1–18 grains
TQ.7	Small lense	418	60°	75°	8.37	0.691	Pyrite in small amount to 5%, chalcopryrite 1–10%, pyrrhotite in small amount to 8%, cubanite 1–10%, covellite in small amount to 3%, rutile a few grains, limonite in small amount to 5%
TQ.8	Vein	270	60°	75°	5.53	0.587	Pyrite in small amount, chalco-pyrite 15%, melnikovite in small amount, cubanite in very small amount to 1%, covellite 1%, limonite 1%
TQ.9a	Large lense	735	65°	65°	13.61	0.530	Pyrrhotite 10–18%, chalcopryrite in small amount to 2%, graphite in small amount to 3%, cubanite in very small amount, sphene a few grains
TQ.9b	Large lense	640	60°	60°	9.96	0.516	Pyrrhotite in very small amount to 10%, chalcopryrite 0.5–12%, pyrite 2%, arsenopyrite 1%, graphite in small amount, cubanite very scarce, sphene a few grains, covellite in small amount, and limonite 0.5%.
TQ.10	Small lense	340	50°	70°	11.69	0.568	Pyrrhotite in very small amount to 8%, chalcopryrite 1%, mag-netite 3%, ilmenite 1–2%
TQ.10a	Small lense	190	50°	70°	13.79	0.763	Pyrrhotite 30%, chalcopryrite 4%, graphite 7%, pyrite 1%, sphalerite in very small amount
TQ.11	Vein	718	60°	65°	4.77	0.674	Pyrrhotite 2–6%, chalcopryrite 1%, graphite 2%, sphene a few grains, sphalerite in very small amount
TQ.13	Vein	400	65°	70°	3.09	0.481	Pyrite in very small amount to 2%, chalcopryrite 1–10%, graph-ite 1–2%, marcasite in very small amount to 3%, covellite in small amount, rutile in small amount

Chalcopyrite (CuFeS_2): The most abundant copper-bearing mineral, occurring as anhedral to subhedral grains with sizes ranging from 0.1 to 2 mm, typically between 0.1 and 1 mm. Chalcopyrite commonly exhibits disseminated, vein, and replacement textures, forming intergrowths with pyrite and pyrrhotite (Figs. 3, *a*, *b*). Under the microscope, chalcopyrite is characterized by its straw-yellow color with moderate reflectance.

Bornite (Cu_5FeS_4): Occurs as fine-grained disseminations or as replacement rims around chalcopyrite.

In some samples, bornite is partially replaced by covellite, indicating secondary enrichment (Figs. 3, *n*, *o*). It exhibits a distinct purplish-brown to reddish hue under the microscope.

Pyrite (FeS_2): Present as euhedral to subhedral grains, ranging in size from 0.1 to 2 mm, often forming intergrowths with chalcopyrite. Pyrite is commonly replaced by chalcopyrite and bornite along fractures and grain boundaries (Figs. 3, *e*, *f*). Under reflected light, pyrite appears bright yellow with high reflectance.

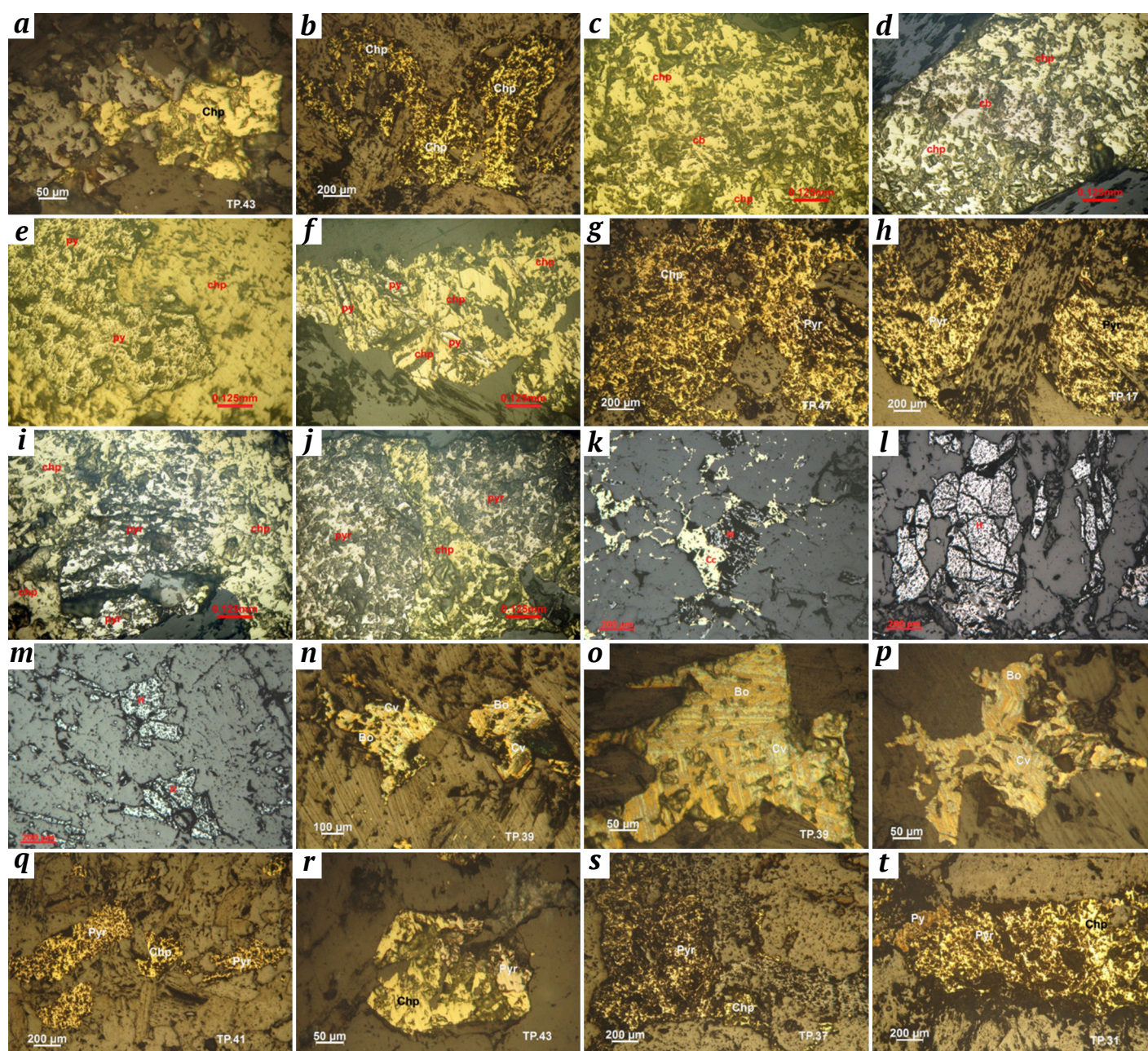


Fig. 6. Primary copper ore mineral assemblage in the Ta Phoi deposit:

a, *b* – disseminated chalcopyrite in a gangue matrix; *c*, *d* – syngenetic relationship between chalcopyrite and cubanite; *e* – chalcopyrite replacing pyrite; *f* – disseminated chalcopyrite and pyrite in an ore matrix; *g*, *h*, *i*, *j* – disseminated chalcopyrite and pyrrhotite in a gangue matrix; *k* – euhedral chalcopyrite grains replacing magnetite; *l*, *m* – subhedral hematite grains forming clusters within the rock matrix; *n*, *o*, *p* – bornite replaced by covellite through corrosive processes; *q*, *r*, *s*, *t* – euhedral chalcopyrite and pyrrhotite disseminated within the rock matrix



Pyrrhotite (Fe_{1-x}S): Found as anhedral grains up to 2 mm in size, often occurring in association with chalcopyrite and cubanite. Pyrrhotite grains exhibit weak anisotropy and are commonly replaced by later-stage sulfides (Figs. 3, *g, h, i, j*).

Cubanite (CuFe_2S_3): A minor phase in the ore, appearing as thin lamellar intergrowths within chalcopyrite. Cubanite has a darker yellow color with a faint pinkish tint under the microscope (Figs. 3, *c, d*).

Magnetite (Fe_3O_4): Occurs as fine, scattered grains within the ore, often showing replacement by chalcopyrite (Fig. 3, *k*).

Secondary ore minerals are covellite, chalcocite, limonite, and malachite.

Covellite (CuS): Originates as a supergene product replacing chalcopyrite and bornite, often appearing as deep blue rims around primary sulfides (Fig. 3, *p*).

Chalcocite (Cu_2S): Found in small amounts, typically replacing chalcopyrite in oxidation zones. It appears as a fine-grained, dark gray mineral with a metallic luster.

Limonite ($\text{FeO}(\text{OH}) \cdot n\text{H}_2\text{O}$): It is widespread in oxidation zones, pseudomorphically replacing pyrite and chalcopyrite. It is commonly associated with goethite and hematite.

Malachite [$\text{Cu}_2(\text{OH})_2\text{CO}_3$]: Occurs as green botryoidal crusts, often coating surfaces of fractures and voids within altered host rocks.

The results of mineralogical sample analysis indicate that the Ta Phoi deposit exhibits the following common ore textures and structures.

Disseminated and clustered structures: These are the most common structures observed in the ore bodies, where chalcopyrite, pyrite, pyrrhotite, and cubanite are dispersed as fine to medium-grained aggregates in the host rock matrix (Figs. 3, *q, r, s, t*). The distribution of ore minerals is irregular, with forming clusters of variable sizes within altered host rocks.

Massive structure: Pyrite, pyrrhotite, and chalcopyrite frequently occur as compact massive aggregates, forming sulfide-rich zones. These zones often appear as coarse-grained, tightly packed sulfides, replacing earlier mineral phases (Figs. 3, *c, e*).

Vein and stringer structures: Hydrothermal replacement and infill processes have resulted in the formation of sulfide-bearing veins and micro-veinlets, composed mainly of chalcopyrite, pyrrhotite, and minor chalcocite. These veinlets exhibit variable thicknesses and cut across the host rock, often filling fractures and microfractures (Fig. 3, *t*).

Replacement and corrosion structures: Secondary enrichment zones show formation of covellite, chalcocite, limonite, and goethite replacing and

corroding primary sulfides such as chalcopyrite and pyrrhotite. These minerals form rims around the primary sulfides, indicating manifestations of oxidation and supergene processes (Figs. 3, *i, l*).

Euhedral to subhedral grain texture: Chalcopyrite and pyrite frequently exhibit well-developed crystal faces, indicating crystallization under favorable conditions. This texture is more commonly observed in primary mineralization zones.

Anhedral grain texture: A prevalent texture in the sulfide ores, where chalcopyrite, pyrrhotite, and cubanite display irregular, intergrown morphologies due to replacement and overgrowth processes.

Colloform texture: Observed mainly in secondary minerals such as marcasite, melnikovite, and covellite, forming concentric layers around pre-existing sulfides. This texture suggests low-temperature hydrothermal precipitation.

Residual texture: Early-formed sulfides, such as pyrite and pyrrhotite, are partially replaced by younger sulfides like chalcopyrite and bornite, leaving behind embayed and corroded outlines.

Brecciated and fragmented texture: In faulted and sheared zones, sulfide minerals appear fragmented and cemented by later-stage hydrothermal minerals, forming breccia-like textures.

2.5.2. Paragenetic sequence

Based on the geological conditions of ore formation, the morphological relationships of minerals within the ore, and their genetic morphological characteristics, it is possible to identify characteristic mineral associations as well as the ore-forming periods and stages present in the study area. A summarized mineral associations are provided in Table 2.

The hydrothermal period consists of three ore-forming stages. Early stage is dominated by the formation of disseminated quartz and magnetite with minor pyrite. Main sulfide stage is characterized by origination of sulfide minerals, forming a mineral association of pyrite, pyrrhotite, chalcopyrite, and cubanite alongside quartz. The mineralization occurs predominantly as disseminated grains, with minor development in veinlets. Post ore stage represents the principal phase of copper ore formation. This stage produces a quartz–chalcopyrite–cubanite association, accompanied by extensive hydrothermal alteration of the host rocks, including epidotization, actinolitization, tremolization, and chloritization.

The supergene enrichment period consists of a single ore-forming stage, characterized by covellinization, chalcocitization, and limonitization of primary ore minerals (see Table 2).



Table 2

Mineral associations at the Ta Phoi deposit, northwestern Vietnam

Minerals	Hydrothermal mineralization			Epigenesis
	Quartz – mag-netite	Quartz – pyrite	Quartz – chalcopyrite – cubanite	Covellite – chalcocite – limonite
Quartz				
Magnetite	— — — — —	— — — — —		
Pyrite		— — — — —	— — — — —	
Molybdenite		— — — — —		
Chalcopyrite			— — — — —	
Cubanite			— — — — —	
Pyrrhotite			— — — — —	
Melnikovite			
Chalcocite				— — — — —
Covellite				— — — — —
Goethite				— — — — —
Hydrogoethite				— — — — —
Limonite				— — — — —

— — — — — Main (>5%)
 — — — — — Minor (1–5%)
 Locally occurring

3. Sampling and analytical methods

3.1. Study material and petrography observation

This study used sulfide copper ore samples and associated gangue minerals, including sphene and quartz, collected from both surface and subsurface exposures of the Ta Phoi deposit. Selected samples were prepared as polished sections and observed under optical microscopy and Scanning Electron Microscopy (SEM) for mineral identification, textural relationships, and alteration features of sphene and associated minerals.

3.2. Analytical methods

3.2.1. SEM analysis

SEM study was conducted using an FEI Quanta 200 microscope equipped with an EDS system at 20 kV and 20 nA. Back-scattered electron (BSE) imaging was applied to study zoning, morphology, and alteration features of sphene. Analyses were performed at the National Key Laboratory, China University of Geosciences (Wuhan).

3.2.2. Fluid inclusion microthermometry

Doubly polished quartz sections (~0.20 mm thick) were analyzed using a Linkam THMSG 600 heating-freezing stage mounted on an Olympus BX51 microscope. The fluid inclusion study was focused on primary, pseudosecondary, and secondary inclusions based on established classification criteria [49, 50]. Eutectic and melting temperatures were used to estimate salinity and fluid density, with calculations performed using the FLINCOR software. Temperature accuracy was ±0.2°C between –20°C and +20°C.

3.2.3. Sulfur isotope analysis

Sulfur isotope measurements were conducted using a Delta V Plus mass spectrometer at the CNNC Beijing Research Institute of Uranium Geology. Results are reported in $\delta^{34}\text{S}$ values relative to the V-CDT standard, with analytical precision better than ±0.2‰ (2σ).

3.2.4. U-Pb isotope analysis of sphene

U-Pb dating of sphene was conducted at the State Key Laboratory of Geological Processes and Mineral Resources (GPMR), China University of Geosciences (Wuhan), using an Agilent 7700x ICP-MS system coupled with a GeoLas 2005 laser-ablation system equipped with a DUV 193 nm ArF-excimer laser. Analytical procedures and data reduction methods followed those described by Spandler et al. (2016) [51]. A laser spot size of 32 μm was used for all analyses, with ^{43}Ca serving as the internal standard isotope, previously measured by EPMA. NIST SRM610 was used as a bracketing external standard [51]. The laser fluence was set at 5 J/cm², with a repetition rate of 10 Hz, the parameters optimized to enhance analytical sensitivity while minimizing elemental fractionation. Calibration of geochemical and isotopic data was achieved by performing one measurement of MKED1 and NIST SRM610 after every three ordinary sample analyses. The MKED1 reference material originates from the Elaine Dorothy Cu-Au-REE deposit in the Mount Isa Inlier, Queensland, Australia. Concordia diagrams and $^{206}\text{Pb}/^{238}\text{U}$ weighted mean age calculations were generated using Isoplot/Ex_ver3 [52].

4. Results and Discussions

4.1. Sulfur isotopic compositions of sulfide minerals

The analytical results of sulfide samples are summarized in Table 3. This study determined the $\delta^{34}\text{S}$ values for five chalcopyrite samples and one pyrite sample from the Ta Phoi deposit. The sulfur isotope compositions of these six samples range from +2.2‰ to +3.1‰, with an average of +2.85‰.

The sulfur isotope analyses of chalcopyrite and pyrite from the Ta Phoi deposit showed a narrow range close to 0‰, which is consistent with the mantle-derived sulfur signature (Fig. 7). This suggests that the source of ore-forming materials in the Ta Phoi copper deposit was relatively homogeneous magmatic reservoir.

4.2. Ore-forming fluids

Analyses of 8 quartz samples associated with copper ore identified 97 fluid inclusions with elliptical, triangular, or elongated elliptical morphologies. These inclusions are classified into two types: liquid-vapor (type I) and $\text{CO}_2\text{-H}_2\text{O}$ vapor inclusions (type II) (Table 4). Among them, type I inclusions (from 6 quartz samples) account for 77 inclusions, while type II inclusions (from 2 quartz samples) comprise 20 inclusions. Microthermometric measurements of the homogenization temperatures for type I (liquid-vapor) inclusions range from 163.1 to 375.6°C, with an average of 256.4°C. The dominant temperature range was 240–300°C. The freezing point temperatures vary between –10.5 and –1.0°C, predominantly between –5.0 and –3.0°C. For type II ($\text{CO}_2\text{-H}_2\text{O}$) inclusions,

Table 3

Sulfur isotope compositions of chalcopyrite and pyrite crystals from ore samples of the Ta Phoi deposit

No.	Sample	Location	Mineral	$\delta^{34}\text{S}_{\text{V-CDT}}$	2 σ
1	TP-01	Surface, TQ.4	Chalcopyrite	2.6	0.2
2	TP-02	Surface, TQ.5	Chalcopyrite	2.4	0.2
3	TP-03	Surface, TQ.6	Chalcopyrite	2.2	0.2
4	TP-04	30m below surface, TQ.4	Chalcopyrite	2.9	0.2
5	TP-05	50m below surface, TQ.6	Chalcopyrite	3.1	0.2
6	TP-06	120m below surface, TQ.6	Pyrite	3.9	0.1
Average				2.85	

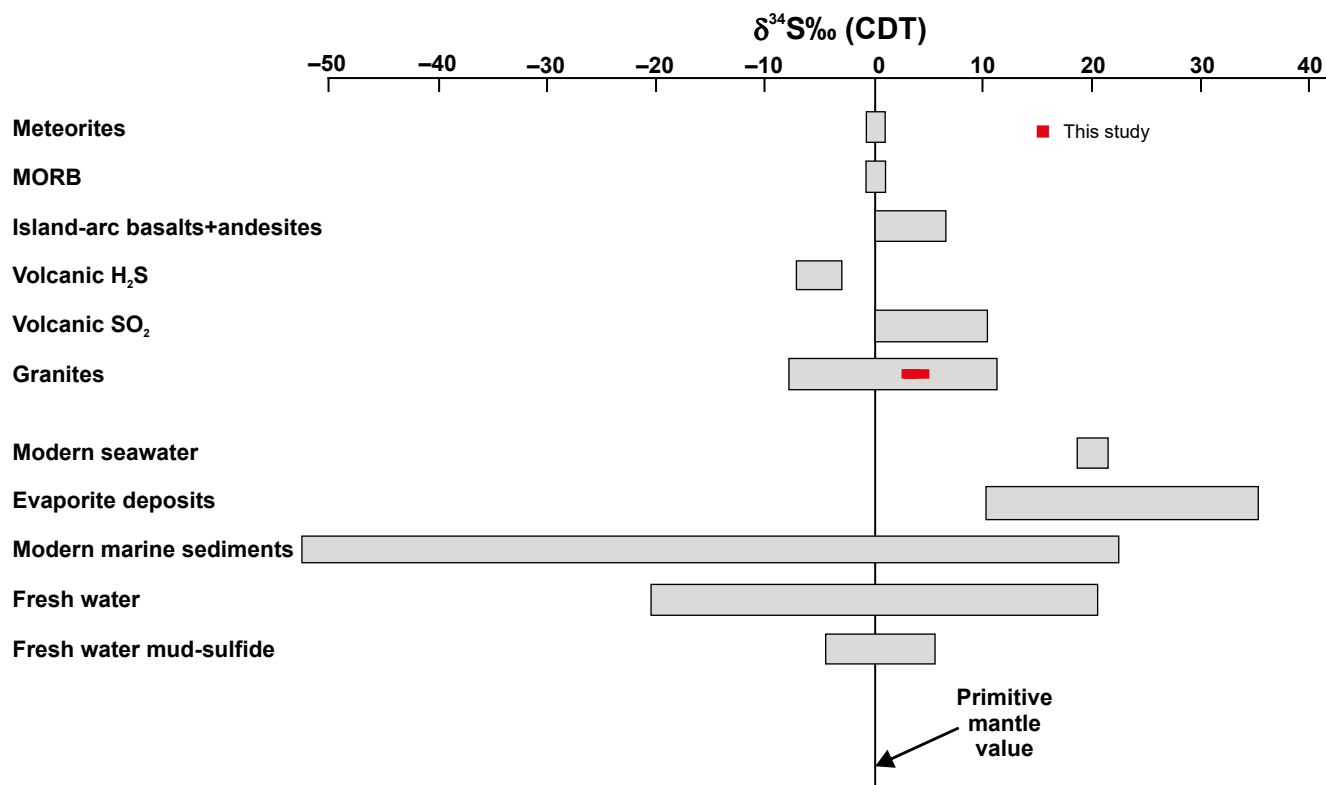


Fig. 7. Natural sulfur isotope reservoirs, showing copper forming material sources in the Ta Phoi deposit (data from [53–59])



homogenization temperatures range from 250 to 410°C, with an average of 350°C. The dominant temperature range was 330–360°C. The freezing point temperatures vary from –11.8 to –3.8°C, mostly between –6.2 and –4.8°C. The salinity of the fluid inclusions ranges from 2.1 to 16.25 wt %, with the majority falling between 4.0 and 6.6 wt %, and an average of 6.96 wt %. The fluid density ranges from 1.15 to 1.91 g/cm³, with an average of 1.35 g/cm³.

The fluid inclusion analyses indicated that the measured homogenization temperatures ranged from 163.1°C to 410°C, with a dominant range of 250°C to 350°C, classifying the ore-forming fluids as medium to relatively high temperature. The salinity values ranged from 2.1% to 16.25%, indicating a moderate salinity level. The ore-forming pressure varied between 43.98 and 99.85 MPa, while the formation depth ranged from 3.39 to 6.45 km, suggesting that the ore was formed at an intermediate depth.

4.3. Timing of copper mineralization

The U-Pb dating results for two samples of sphene are presented with the corresponding concordia diagrams shown in Fig. 8. In sample TP-12, 25 spot analyses performed on 10 sphene grains yielded concordant U-Pb ages, with a weighted average ²⁰⁶Pb/²³⁸U age of 810.7 ± 4.6 Ma (*n* = 25, MSWD = 0.82). Similarly, for sample TP-19, 25 spot analyses on 12 sphene grains produced concordant U-Pb ages, yielding a weighted average ²⁰⁶Pb/²³⁸U age of 819.5 ± 2.0 Ma (*n* = 25, MSWD = 5.2).

The U-Pb dating of sphene from the Ta Phoi copper deposit indicates that mineralization occurred between 810 and 820 Ma (Fig. 8). This age is comparable to the emplacement age of 860–740 Ma for granodiorite and diorite bodies such as the Phin Ngan, Suoi Thau, and Lung Thang massifs [11, 47, 65]. The spatial proximity of these intrusions to the Ta Phoi deposit suggests a genetic link between the copper mineralization and magmatic activity.

4.4. Origin and formation conditions

The Ta Phoi deposit is interpreted as a medium- to high-temperature hydrothermal-metasomatic deposit with a magmatic source of ore-forming materials. Copper ores are confined to the contact between the Sin Quyen Formation and hornblende diorite intrusions. They are mainly concentrated within altered rocks (with minor occurrences in quartz-feldspar-biotite schist) and are associated with a characteristic mineral association of tremolite-actinolite, albite, and epidote.

Moreover, the spatial proximity of the Neoproterozoic Phin Ngan, Suoi Thau, and Lung Thang granodiorite and diorite massifs to the Ta Phoi deposit suggests a potential genetic relationship between the two. This implies that the formation of the Ta Phoi deposit may have been influenced by tectonic processes associated with these magmatic intrusions. Specifically, the Phin Ngan, Suoi Thau, and Lung Thang massifs, which were formed in a subduction-related continental arc setting [11, 42, 47], may have played a crucial role in the mineralization process.

Table 4

Сводка данных по флюидным включениям на месторождении Та Фой

Sample	Type of inclusion	Quantity	$T_{m,ice}$, °C (mean)	T_h , °C (mean)	Salinity, wt % NaCl (mean)	Density, g/cm ³ (mean)	Pressure, MPa (mean)	Depth, km (mean)
TP-I.1	Type I	12	–2.9––2.1 (–2.53)	290–321 (304.5)	2.1–8.68 (5.19)	1.15–1.54 (1.29)	43.98–95.13 (66.56)	3.46–6.23 (4.76)
TP-I.2		14	–5.2––1.0 (–2.95)	163,1–372 (335.0)	3.06–14.25 (6.13)	1.16–1.68 (1.31)	44.53–99.85 (68.43)	3.50–6.45 (4.86)
TP-I.3		15	–10.5––2.3 (–3.94)	272–375,6 (314.24)	2.42–14.15 (7.42)	1.15–1.59 (1.32)	47.36–94.52 (69.70)	3.67–6.20 (4.93)
TP-I.4		12	–5.0––2.5 (–3.51)	240–350 (308.33)	4.63–11.55 (7.31)	1.13–1.51 (1.33)	46.06–93.44 (70.27)	3.39–6.15 (4.94)
TP-I.5		15	–5.1––2.5 (–4.21)	210–310 (266.67)	6.73–15.16 (9.99)	1.16–1.41 (1.29)	47.65–77.01 (64.18)	3.69–5.35 (4.65)
TP-I.6		9	–4.2––1.5 (–3.16)	170–285 (230.44)	7.02–16.05 (10.77)	1.18–1.47 (1.31)	49.19–87.55 (66.45)	3.79–5.87 (4.77)
TP-I.7	Type II	8	–11.8––3.8 (–5.81)	250–410 (333.5)	6.31–16.15 (11.62)	1.19–1.56 (1.35)	50.89–89.41 (69.94)	3.89–5.96 (4.96)
TP-I.8		12	–10.5––4.0 (–5.63)	280–405 (340.58)	7.73–16.25 (11.31)	1.20–1.91 (1.53)	48.34–91.69 (68.10)	3.73–6.07 (4.85)

Note: Salinities and density were calculated using the method proposed by [60, 61]; pressures were calculated using the method proposed by [62]; depths were estimated using the method proposed by [63,64]; $T_{m,ice}$ – final melting temperature of ice; T_h – homogenization temperature.

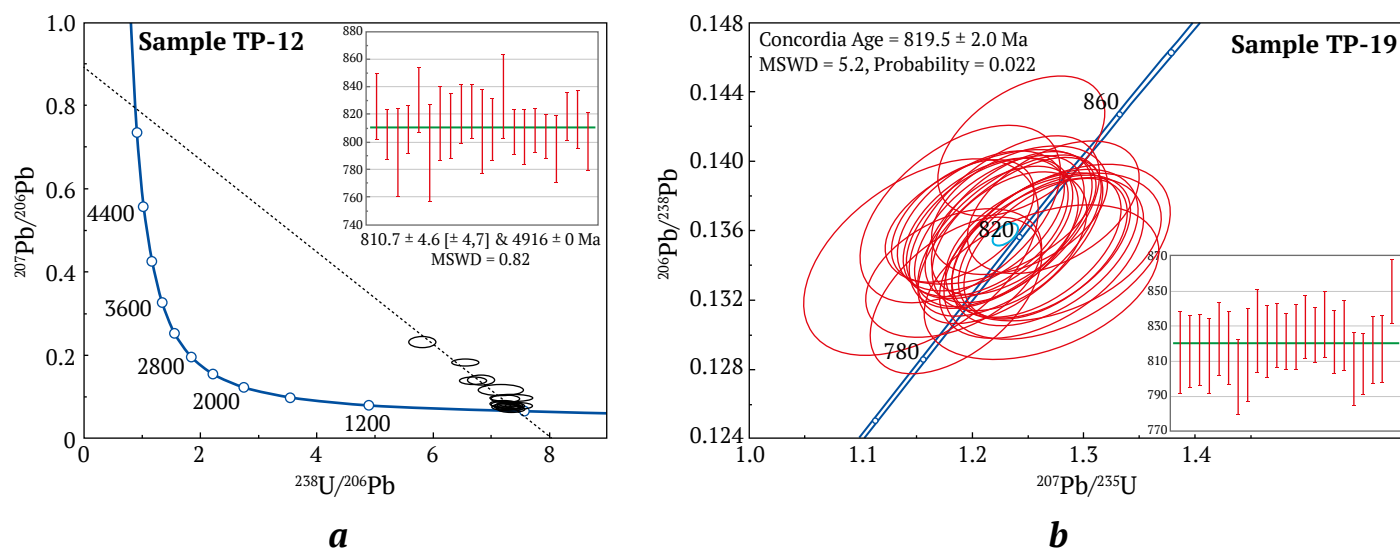


Fig. 8. Concordia diagrams for U-Pb isotopic dating of sphene from the Ta Phoi copper deposit:
a – Sample TP-12 (ore body TQ.4); b – Sample TP-19 (ore body TQ.6)

4.5. Comparison with well-studied porphyry copper deposits

The sulfur isotopic signatures (+2.2‰ to +3.1‰, average +2.85‰) observed in the Ta Phoi copper deposit fall within the typical range for mantle-derived sulfur, which is commonly reported in porphyry copper systems worldwide [66, 67]. For instance, sulfur isotopic values between 0‰ and +5‰ have been documented in sulfide minerals from porphyry Cu-Mo deposits in the Andes (e.g., Chuquicamata, El Teniente) [68], where magmatic sources dominate sulfur input. This consistency suggests that the Ta Phoi deposit, like classic porphyry systems, is also sourced from a relatively homogeneous magmatic reservoir.

In terms of fluid inclusion characteristics, the homogenization temperatures (163–410°C, dominant range 250–350°C) and salinities (2.1–16.25 wt % NaCl equivalent, averaging ~7 wt %) observed in the Ta Phoi deposit are comparable to those reported in porphyry copper systems globally [66–68]. For example, studies on the Batu Hijau (Indonesia) deposits have recorded similar fluid inclusion temperature ranges (250–400°C) and moderate to high salinities (3–16 wt % NaCl), indicative of magmatic-hydrothermal fluids undergoing phase separation and cooling during ore formation [69]. The depth estimates of 3.4–6.5 km at pressures of up to ~100 MPa in the Ta Phoi also align with typical porphyry copper deposit formation depths (2–6 km), further reinforcing this interpretation.

Additionally, the temporal constraint provided by U-Pb sphene ages (810–820 Ma) suggests that the Ta Phoi deposit formed synchronously with nearby Neoproterozoic magmatic intrusions (e.g., Phin Ngan,

Lung Thang, Suoi Thau). This timing of mineralization, spatial proximity, and geochemical affinity (e.g., sulfur isotope signatures, fluid composition) resemble the temporal and spatial relationships commonly observed between porphyry copper deposits and their causative intrusive bodies.

Taken together, the geological, geochemical, and fluid inclusion evidences from the Ta Phoi deposit collectively point to a magmatogene-hydrothermal origin, consistent with characteristics of porphyry copper systems. However, the dominant structural control and hydrothermal-metasomatic features observed in the deposit suggest that the deposit may represent a porphyry-related skarn or endoskarn system developed in response to magmatogene fluid migration along lithological and structural contacts.

4.6. Copper ore exploration potential and metallogenic implications

Data from the Phan Si Pan zone (including Sin Quyen, Ta Phoi, Phin Ngan, Lung Thang, and Suoi Thau deposits) suggest a major metallogenic event between 810 and 820 Ma.

U-Pb dating of granitoids across the zone and along the Ailao Shan–Red River belt confirms synchronous magmatism and mineralization [11, 65], pointing to a shared metallogenic system.

Given the wide distribution of granodiorite–diorite intrusions and their apparent link to the copper mineralization, the region holds high potential for additional undiscovered resources. In particular, areas such as Lung Thang and Suoi Thau remain underexplored and require further investigation.



Conclusions

This study enhances understanding of the Ta Phoi copper deposit through an integrated petrographic, geochemical, isotopic, and geochronological approach. The main findings are as follows:

Firstly, copper occurs in lensoid and vein-type bodies along NW-SE-trending structures. The ore association of chalcopyrite, bornite, pyrite, pyrrhotite, cubanite, and magnetite forms disseminated, anhedral- to subhedral-grained textures that record hydrothermal infilling and replacement.

Secondly, sulfur isotope compositions ($\delta^{34}\text{S}$) values for chalcopyrite and pyrite are magmatic in nature, pointing to nearby granodiorite-diorite intrusions (Phin Ngan, Suoi Thau, and Lung Thang massifs) as the primary metal and fluid reservoirs being sources of the deposit material.

Thirdly, U-Pb ages of hydrothermal sphene (819.5 ± 2.0 to 810.7 ± 4.6 Ma) fix the mineralizing

event in the Neoproterozoic and coincide with the age of intruding the regional intrusive suites, confirming a genetic link.

Furthermore, fluid inclusion microthermometry indicates moderate to high temperatures ($163\text{--}410\text{ }^{\circ}\text{C}$), moderate salinities (7–16 wt % NaCl eq.), trapping depths of $\sim 3.4\text{--}6.5$ km, and pressures of 44–100 Mpa, i.e. conditions typical of magmatogene hydrothermal systems.

Lastly, the magmatic sulfur signature, high-temperature saline fluids, and structural setting together suggest that Ta Phoi deposit represents a porphyry-related skarn (endoskarn) developed in a subduction-related convergent margin during the Neoproterozoic.

Collectively, these results refine the metallogenic framework of the Ta Phoi district and underscore its potential for further copper exploration in north-wester Vietnam.

References

1. Evans A.M. *Ore geology and industrial minerals: an introduction*. 3rd ed. Wiley-Blackwell; 1993. 403 p.
2. Misra K.C. *Understanding ore deposits*. Kluwer Academic Publishers; 2000. 845 p.
3. Robb L. *Introduction to Ore-Forming Processes*. Blackwell Publishing, Oxford; 2004. 373 p.
4. Tri T.V., Khuc V. (eds.) *Geology and earth resources of Vietnam*. General Department of Geology, and Minerals of Vietnam. Hanoi: Publishing House for Science and Technology; 2011. 645 p.
5. Fromaget J. *Études géologiques sur le Nord-Ouest du Tonkin et le Nord du Haut-Laos*. Hanoi; Service Géologique de l'Indochine; 1937. 153 p.
6. Thi P.T. Iron- and copper-bearing metasomatic rocks in the Lao Cai area. *Journal of Geology, Series A*. 1964;32(4):9–15. (In Vietnamese). URL: <http://idm.gov.vn/Data/TapChi/1964/A323.htm>
7. Hai T.Q. Further insights into ore-bearing metasomatic rocks in Sin Quyen. *Journal of Geology, Series A*. 1969;85–86(5–8):23–40. (In Vietnamese). URL: <http://idm.gov.vn/Data/TapChi/1969/a854.htm>
8. Cuong H.H., Han N.D. Ore-forming types in the Sin Quyen area. *Journal of Geology, Series A*. 1969;81–82(12):23–32. (In Vietnamese). URL: <http://idm.gov.vn/Data/TapChi/1969/a813.htm>
9. Mclean R.N. *The Sin Quyen iron oxide-copper-gold-rare earth oxide mineralization of North Vietnam*. In: Porter T.M. (Ed.) *Hydrothermal iron oxide copper-gold & related deposits: a global perspective. Volume 2*. Adelaide: PGC Publishing; 2001. Pp. 293–301.
10. Li X.C., Zhou M.F., Tran M.D. REE mineralization in the Sin Quyen Fe-Cu-LREE-(U-Au) deposit, Northwest Vietnam. In: *Abstracts of the Joint Assembly AGU-GAC-MAC-CGU*. Montreal, Canada; 2015.
11. Dung T.M., Luat N.Q., Hai T.T., et al. *Nature and formation age of copper mineralization in the northeastern Fan Si Pan belt and its metallogenic significance*. Fundamental research project in natural sciences, Code 105.01-2012.06, Ministry of Science and Technology; 2016. 50 p. (In Vietnamese).
12. Dac N.X., Zhao X.F., Hai T.T., et al. Two episodes of REEs mineralization at the sin quyen IOCG deposit, NW Vietnam. *Ore Geology Reviews*. 2020;125:103676. <https://doi.org/10.1016/j.oregeorev.2020.103676>
13. Anh T.T., Dung P.T., Hoa T.T., et al. 2010. *Enhancing mineral extraction efficiency and environmental protection: Investigating associated components in basic metal and rare earth mineral deposits in northern Vietnam*. State Science & Technology Programme, code KC.08.24/06-10. 459 p. (In Vietnamese).
14. Anh B.X. (Ed.) *Report on the assessment of copper ore potential and other mineral resources in the Ta Phoi area, Cam Duong Town, Lao Cai Province*. Hanoi: Intergeo Federation; 2007. (In Vietnamese).
15. San P.V. (Ed.). *Exploration report on copper ore in the Ta Phoi area, Lao Cai City, Lao Cai Province*. Hanoi: Geological Information and Archive Center; 2012. (In Vietnamese).
16. Metcalfe I. Permian tectonic framework and palaeogeography of SE Asia. *Journal of Asian Earth Sciences*. 2002;20(6):551–566. [https://doi.org/10.1016/S1367-9120\(02\)00022-6](https://doi.org/10.1016/S1367-9120(02)00022-6)



17. Metcalfe I. Palaeozoic and Mesozoic tectonic evolution and palaeogeography of East Asian crustal fragments: The Korean Peninsula in context. *Gondwana Research*. 2006. 9(1):24–46. <https://doi.org/10.1016/j.gr.2005.04.002>
18. Golonka J., Krobicki M., Paják J, et al. *Global plate tectonics and paleogeography of Southeast Asia*. Faculty of Geology, Geophysics and Environmental Protection. Arkadia, Kraków: AGH-University of Science and Technology; 2006. 128 p.
19. Hung K. T. Overview of magmatism in northwestern Vietnam. *Annales Societatis Geologorum Poloniae*. 2010;80(2):185–226. URL: http://www.asgp.pl/80_2_185_226
20. Pham T.H., Chen F., Wang W., et al. Zircon U-Pb ages and Hf isotopic composition of the Posen granite in northwest Vietnam. *Acta Petrologica Sinica*. 2009;25(12):3141–3152. (In Chinese with English abstract). URL: http://www.ysxb.ac.cn/en/article/id/aps_20091204
21. Wang W., Cawood P.A., Zhou M. F., Zhao J. H. Paleoproterozoic magmatic and metamorphic events link Yangtze to northwest Laurentia in the Nuna supercontinent. *Earth and Planetary Science Letters*. 2016;433:269–279. <https://doi.org/10.1016/j.epsl.2015.11.005>
22. Qi X., Santosh M., Zhao Y., et al. Mid-Neoproterozoic ridge subduction and magmatic evolution in the northeastern margin of the Indochina block: Evidence from geochronology and geochemistry of calc-alkaline plutons. *Lithos*. 2016;248–251:138–152. <https://doi.org/10.1016/j.lithos.2015.12.028>
23. Minh P., Hieu P.T., Thuy N.T.B., et al. Neoproterozoic granitoids from the Phan Si Pan Zone, NW Vietnam: Geochemistry and geochronology constraints on reconstructing South China–India Palaeogeography. *International Geology Review*. 2021;63(5):585–600. <https://doi.org/10.1080/00206814.2020.1728584>
24. Polyakov G., Balykin P., Hoa T.T., et al. Evolution of the Mesozoic-Cenozoic magmatism of the Song Da rift and its contouring structures. *Geologiya i Geofizika*. 1998;39(6):695–706. (In Russ.)
25. Anh T.V., Pang K.N., Chung S.L., et al. The Song Da magmatic suite revisited: A petrologic, geochemical and Sr–Nd isotopic study on picrites, flood basalts and silicic volcanic rocks. *Journal of Asian Earth Sciences*. 2011;42(6):1341–1355. <https://doi.org/10.1016/j.jseaes.2011.07.020>
26. Metcalfe I. Changhsingian (late Permian) conodonts from Son La, northwest Vietnam and their stratigraphic and tectonic implications. *Journal of Asian Earth Sciences*. 2012;50:141–149. <https://doi.org/10.1016/j.jseaes.2012.01.002>
27. Faure M., Lepvrier C., Van Nguyen V., et al. The South China block–Indochina collision: Where, when, and how? *Journal of Asian Earth Sciences*. 2014;79(Part A):260–274. <https://doi.org/10.1016/j.jseaes.2013.09.022>
28. Faure M., Lin W., Chu Y., Lepvrier C. Triassic tectonics of the southern margin of the South China block. *Comptes Rendus Geoscience*. 2016;348(1):5–14. <https://doi.org/10.1016/j.crte.2015.06.012>
29. Minh P., Hieu P.T., Hoang N.K. Geochemical and geochronological studies of the Muong Hum alkaline granitic pluton from the Phan Si Pan Zone, northwest Vietnam: Implications for petrogenesis and tectonic setting. *The Island Arc*. 2018;27(4):12250. <https://doi.org/10.1111/iar.12250>
30. Usuki T., Lan C.Y., Tran T.H., et al. Zircon U–Pb ages and Hf isotopic compositions of alkaline silicic magmatic rocks in the Phan Si Pan-Tu Le region, northern Vietnam: Identification of a displaced western extension of the emeishan large igneous province. *Journal of Asian Earth Sciences*. 2015;97(Part A):102–124. <https://doi.org/10.1016/j.jseaes.2014.10.016>
31. Tran T.H., Lan C.Y., Usuki T., et al. Petrogenesis of late permian silicic rocks of Tu Le basin and Phan Si Pan uplift (NW Vietnam) and their association with the Emeishan large igneous province. *Journal of Asian Earth Sciences*. 2015;109:1–19. <https://doi.org/10.1016/j.jseaes.2015.05.009>
32. *Geology of Vietnam: Stratigraphy*. DGMVN (Department of Geology and Minerals of Vietnam). Hanoi: Science Publisher; 1995. 359 p. (In Vietnamese).
33. Pham T.H., Lei W.X., Minh P., et al. Archean to Paleoproterozoic crustal evolution in the Phan Si Pan zone, Northwest Vietnam: Evidence from the U-Pb geochronology and Sr–Nd–Hf isotopic geochemistry. *International Geology Review*. 2022;64(1):96–118. <https://doi.org/10.1080/00206814.2020.1839976>
34. Lan C.Y., Chung S.L., Lo C.H., et al. First evidence for Archean continental crust in northern Vietnam and its implications for crustal and tectonic evolution in Southeast Asia. *Geology*. 2001;29(3):219–222. [https://doi.org/10.1130/0091-7613\(2001\)029<0219:FEFACC>2.0.CO;2](https://doi.org/10.1130/0091-7613(2001)029<0219:FEFACC>2.0.CO;2)
35. Nam T.N. 750 Ma U–Pb zircon age of the Po Sen Complex and tectonic implication. *Journal of Geology*. 2003;274:11–16. (In Vietnamese). URL: <http://idm.gov.vn/Data/TapChi/2003/274/t11.htm>
36. Zhao T., Cawood P.A., Wang K., et al. Neoproterozoic and Paleoproterozoic K-rich granites in the Phan Si Pan Complex, North Vietnam: Constraints on the early crustal evolution of the Yangtze Block. *Precambrian Research*. 2019;332:105395. <https://doi.org/10.1016/j.precamres.2019.105395>



37. Zhao T., Cawood P.A., Zi J. W., et al. Positioning the Yangtze Block within Nuna: Constraints from paleoproterozoic granitoids in North Vietnam. *Precambrian Research*. 2023;391:107059. <https://doi.org/10.1016/j.precamres.2023.107059>
38. Wang P.L., Lo C.H., Lan C.Y., et al. 2011. Thermochronology of the PoSen complex, northern Vietnam: Implications for tectonic evolution in SE Asia. *Journal of Asian Earth Sciences*. 2011;40(5):1044–1055. <https://doi.org/10.1016/j.jseaes.2010.11.006>
39. Pham T.H., Chen F.K., Thuy N.T.B., et al. Geochemistry and zircon U–pb ages and Hf isotopic composition of Permian alkali granitoids of the Phan Si Pan zone in northwestern Vietnam. *Journal of Geodynamics*. 2013;69:106–121. <https://doi.org/10.1016/j.jog.2012.03.002>
40. Pham T.T., Shellnutt J.G., Tran T.A., Lee H.Y. Petrogenesis of eocene to early Oligocene granitic rocks in Phan Si Pan uplift area, northwestern Vietnam: Geochemical implications for the Cenozoic crustal evolution of the South China block. *Lithos*. 2020;372:105640. <https://doi.org/10.1016/j.lithos.2020.105640>
41. Dung P.T., Usuki T., Tran H.T., et al. Emplacement ages, geochemical and Sr–Nd–Hf isotopic characteristics of Cenozoic granites in the phan si pan uplift, Northwestern Vietnam: Petrogenesis and tectonic implication for the adjacent structure of the red river shear zone. *International Journal of Earth Sciences*. 2023;112:1475–1497. <https://doi.org/10.1007/s00531-023-02307-4>
42. Li X.C., Zhao J.H., Zhou M.F., et al. Neoproterozoic granitoids from the Phan Si Pan belt, Northwest Vietnam: Implication for the tectonic linkage between Northwest Vietnam and the Yangtze Block. *Precambrian Research*. 2018;309:212–230. <https://doi.org/10.1016/j.precamres.2017.02.019>
43. Zhou M.F., Yan D.P., Kennedy A.K., et al. SHRIMP U–pb zircon geochronological and geochemical evidence for Neoproterozoic arc-magmatism along the western margin of the Yangtze Block, South China. *Earth and Planetary Science Letters*. 2002;196(1–2):51–67. [https://doi.org/10.1016/S0012-821X\(01\)00595-7](https://doi.org/10.1016/S0012-821X(01)00595-7)
44. Zhao J.H., Zhou M.F. Neoproterozoic adakitic plutons in the northern margin of the Yangtze Block, China: Partial melting of a thickened lower crust and implications for secular crustal evolution. *Lithos*. 2008;104(1):231–248. <https://doi.org/10.1016/j.lithos.2007.12.009>
45. Cai Y., Wang Y., Cawood P.A., et al. Neoproterozoic subduction along the Ailaoshan zone, South China: Geochronological and geochemical evidence from amphibolite. *Precambrian Research*. 2014;245:13–28. <https://doi.org/10.1016/j.precamres.2014.01.009>
46. Cai Y., Wang Y., Cawood P.A., et al. Neoproterozoic crustal growth of the Southern Yangtze Block: Geochemical and zircon U–Pb geochronological and Lu–hf isotopic evidence of neoproterozoic diorite from the Ailaoshan zone. *Precambrian Research*. 2015;266:137–149. <https://doi.org/10.1016/j.precamres.2015.05.008>
47. Dac N. X., Khan A., Ullah Z., et al. Neoproterozoic granitoids of northwest Vietnam and their tectonic implications. *International Geology Review*. 2024;66(16):2918–2939. <https://doi.org/10.1080/00206814.2024.2309470>
48. Dung T.M., Liu J.L., Li X.C., Cung D.M. Geology, fluid inclusion and isotopic study of the neoproterozoic Suoi Thau copper deposit, Northwest Vietnam. *Acta Geologica Sinica (English Edition)*. 2016;90(3):913–927. <https://doi.org/10.1111/1755-6724.12733>
49. Roedder E. *Fluid inclusions*. *Reviews in Mineralogy*. 1984;12:1–644.
50. Van den Kerkhof A.M., Hein U.F. Fluid inclusion petrography. *Lithos*. 2001;55(1–4):27–47. [https://doi.org/10.1016/S0024-4937\(00\)00037-2](https://doi.org/10.1016/S0024-4937(00)00037-2)
51. Spandler C., Hammerli J., Sha P., et al. MKED1: A new titanite standard for in situ analysis of SmNd isotopes and U–Pb geochronology. *Chemical Geology*, 2016;425:110–126. <https://doi.org/10.1016/j.chemgeo.2016.01.002>
52. Ludwig K. User's manual for Isoplot/Ex, version 3.00, a geochronological toolkit for Microsoft excel. *Berkeley: Berkeley Geochronology Center Special Publication*; 2003. 70 p.
53. Coleman M.L. Sulphur isotopes in petrology. *Journal of the Geological Society*. 1977;133:593–608. <https://doi.org/10.1144/gsjgs.133.6.0593>
54. Claypool G.E., Helser W.T., Kaplan I.R., et al. The age curves of sulfur and oxygen isotopes in marine sulfate and their mutual interpretation. *Chemical Geology*. 1980;28:199–260. [https://doi.org/10.1016/0009-2541\(80\)90047-9](https://doi.org/10.1016/0009-2541(80)90047-9)
55. Chambers L.A. Sulfur isotope study of a modern intertidal environment and the interpretation of ancient sulfides. *Geochimica et Cosmochimica Acta*. 1982;46(5):721–728. [https://doi.org/10.1016/0016-7037\(82\)90023-0](https://doi.org/10.1016/0016-7037(82)90023-0)



56. Sakai H., Casadevall T.J., Moore J.G. Chemistry and isotope ratios of sulfur in basalts and volcanic gases at Kilauea volcano, Hawaii. *Geochimica et Cosmochimica Acta*. 1982;46(5):729–738. [https://doi.org/10.1016/0016-7037\(82\)90024-2](https://doi.org/10.1016/0016-7037(82)90024-2)
57. Kerridge J.F., Haymon R.M., Kastner M. Sulfur isotope systematics at the 21oN site, East Pacific Rise. *Earth and Planetary Science Letters*. 1983;66:91–100. [https://doi.org/10.1016/0012-821X\(83\)90128-0](https://doi.org/10.1016/0012-821X(83)90128-0)
58. Ueda A., Sakai H. Sulfur isotope study of Quaternary volcanic rocks from the Japanese islands arc. *Geochimica et Cosmochimica Acta*. 1984;48(9):1837–1848. [https://doi.org/10.1016/0016-7037\(84\)90037-1](https://doi.org/10.1016/0016-7037(84)90037-1)
59. Chaussidon M., Albarede F., Sheppard S.M.F. Sulfur isotope variations in the mantle from ion microprobe analyses of micro-sulphide inclusions. *Earth and Planetary Science Letters*. 1989;92(2):144–156. [https://doi.org/10.1016/0012-821X\(89\)90042-3](https://doi.org/10.1016/0012-821X(89)90042-3)
60. Bakker R. *Optimal interpretation of microthermometrical data from fluid inclusions: thermodynamic modelling and computer programming*. Habilitation, Ruprecht-Karls-University; 1999.
61. Bakker R.J., AqSo_NaCl: Computer program to calculate P-T-V-X properties in the H₂O-NaCl fluid system applied to fluid inclusion research and pore fluid calculation. *Computers & Geosciences*. 2018;115:122–133. <https://doi.org/10.1016/j.cageo.2018.03.003>
62. Shao J.L., Mei J.M. On the study of typomorphic characteristics of mineral inclusion in the gold deposit from volcanic terrain in Zhejiang and its genetic and prospecting significance. *Minerals and Rocks*. 1986;3:103–111. (In Chinese with English Abstract).
63. Sibson R.H. Seismogenic Framework for Hydrothermal Transport and Ore Deposition. *Rev. Economic Geology*. 2001;14:25–50. <https://doi.org/10.5382/Rev.14.02>
64. Sibson R.H. Controls on Maximum Fluid Overpressure Defining Conditions for Mesozonal Mineralisation. *Journal of Structural Geology*. 2004;26(6–7):1127–1136. <https://doi.org/10.1016/j.jsg.2003.11.003>
65. Dac N.X., Son T.H., Tin Q.D., et al. In situ U-Pb isotopic dating method on titanite, and application to determine REE-Fe-Cu mineralization age of the Sin Quyen deposit, Lao Cai province. *Journal of Mining and Earth Sciences*. 2023;64(6):50–57. [https://doi.org/10.46326/JMES.2023.64\(6\).06](https://doi.org/10.46326/JMES.2023.64(6).06)
66. Seedorff E., Dilles J.H., Proffett J.M. Jr., et al. Porphyry deposits—characteristics and origin of hypogene features. society of economic geologists. *Economic Geology 100th Anniversary Volume, 1905–2005*. 2005:251–298. <https://doi.org/10.5382/AV100.10>
67. Sillitoe R.H. Porphyry Copper Systems. *Economic Geology*. 2010;105:3–41. <https://doi.org/10.2113/gsecongeo.105.1.3>
68. Berger B.R., Ayuso R.A., Wynn J.C., Seal R.R. *Preliminary model of porphyry copper deposits*. Open-File Report 2008–1321. Reston, VA: U.S. Geological Survey; 2008. 55 p. URL: <https://pubs.usgs.gov/of/2008/1321/>
69. Imai A., Ohno S., Primary ore mineral assemblage and fluid inclusion study of the Batu Hijau Porphyry Cu-Au deposit, Sumbawa, Indonesia. *Resource Geology*. 2008;55(3):239–248. <https://doi.org/10.1111/j.1751-3928.2005.tb00245.x>

Information about the authors

Khuong The Hung – Dr. Sci. (Earth Sci.), Lecturer, Department of Prospecting and Exploration Geology, Hanoi University of Mining and Geology, Hanoi, Vietnam; ORCID [0000-0003-1544-6470](https://orcid.org/0000-0003-1544-6470), Scopus ID [36716173500](https://orcid.org/36716173500); e-mail khuongthehung@humg.edu.vn

Ngo Xuan Dac – Dr. Sci. (Earth Sci.), Researcher, Vietnam Institute of Geosciences and Mineral Resources, Hanoi, Vietnam; e-mail dacbmks@gmail.com

Received 30.03.2025
Revised 14.06.2025
Accepted 16.06.2025